

## Depletion forces in hard-sphere colloids

Riina Tehver,<sup>1</sup> Amos Maritan,<sup>2</sup> Joel Koplik,<sup>3</sup> and Jayanth R. Banavar<sup>1</sup>

<sup>1</sup>*Department of Physics and Center for Materials Physics, Pennsylvania State University, University Park, Pennsylvania 16802*

<sup>2</sup>*International School for Advanced Studies (SISSA), Via Beirut 2-4, 34014 Trieste, Italy*

<sup>3</sup>*Benjamin Levich Institute and Department of Physics, City College of the City University of New York, New York, New York 10031*

(Received 5 May 1998; revised manuscript received 18 November 1998)

A system of monosized hard spheres is studied to elucidate the nature of entropic depletion forces. Our calculations include effective forces between two spheres, a hard sphere and a wall, and the behavior near a step edge and a corner. Qualitative differences between our results and those of the Asakura-Oosawa theory are found. We also demonstrate the nonadditivity of such entropic forces in a simple example.  
[S1063-651X(99)50502-3]

PACS number(s): 82.70.Dd, 65.50.+m

The role entropy plays in condensed matter systems can be counterintuitive [1–5]. One might presume that a crystal is held together by the attractive forces between its constituent molecules, yet it is now well established that a collection of particles interacting with each other via a purely repulsive hard-sphere potential crystallizes at a certain density in order to *increase* its entropy. A similar “surprise” can occur in a binary mixture where the increase in the entropy of one component of the system may force another component towards a greater order. These entropic depletion effects are well known to lead to phase separation in colloids and emulsions of large and small particles with short-range repulsive interactions [1–3], and are relevant in paints and catalytic systems [4]. It is believed that the aggregation of red blood cells related to various illnesses is induced by the entropic forces associated with increased concentrations of protein molecules in blood [5].

In this paper, we demonstrate the complexity of the structure of entropic forces and potentials within the context of the simplest possible system made up of monosized hard spheres. Despite the simplicity of our molecular dynamics simulations, to our knowledge, we present the first direct calculations of these forces. Even though more complex systems have been addressed before using Monte Carlo simulations and analytical theories [6–9], the intrinsic assumptions and approximations present in those methods require independent testing. Depletion forces in complex geometries with step edges [10] and nontrivial curvature [11] have been measured and argued to have profound consequences for cellular biology [11] and entropic control and directed motion of colloidal particles [10]. Our simulations lend themselves easily to different geometries and enable the study of the forces near a step edge and a corner. Finally, we also demonstrate the inherent nonpairwise additive nature of depletion forces.

A successful attempt at predicting and explaining entropic forces was made by Asakura and Oosawa [12] (AO). They consider bodies in a solution of macromolecules or simply a system of larger and smaller particles. Assuming that all of the particles have a hard core, each large particle is surrounded by an exclusion volume where small particles cannot enter. Because the entirely entropic free energy of the small particles depends on the free volume accessible to

them, the configurations where the exclusion volumes of large particles overlap are more favored. Hence, there is a short-range force, pushing the large particles toward each other. A large sphere is pushed toward a wall by a similar mechanism. Quantitative AO calculations ignore the interactions between the small spheres completely, and even though an overall acceptable experimental agreement with the AO prediction has been reported [10,11,13,14], the ideal gas approximation based AO theory does not provide a satisfactory description of entropic potentials and forces in dense colloidal suspensions.

Going beyond the simple geometric arguments of AO requires a detailed theory for the structure of a binary fluid because the entropic potential is obtainable from the inter-species two-point distribution function. Even though significant progress has been made [6–9], this is a difficult task for arbitrary densities and large-sphere–small-sphere diameter ratios either analytically or numerically. Thus, we consider the simplest situation in which all of the spheres are of the same size.

Entropic forces are usually discussed within the context of binary mixtures (they are most useful there) but one can also introduce the concept for a monosized system. There are benefits in doing so. There exist numerous thorough studies of monosized hard-sphere systems. A presentation of the existing well-established information in the framework of depletion forces elucidates many of their general features. For a monosized hard-sphere system, the depletion force,  $F$ , is simply the potential of mean force, which, by itself, can be easily found from the pair-distribution function,  $g$ , as  $F/k_B T = \{\partial \ln[g(x)]/\partial x$ , where  $x$  measures the distance between two spheres [15]. As an example, the force between two spheres, when the packing fraction of the surrounding fluid is  $\phi = 0.45$ , is shown in Fig. 1. One can also measure the force directly in molecular dynamics simulations [16], and our results, from direct force measurements where we register the momentum transfer to a sphere per unit time, are also plotted in the figure. (Throughout the text, the data are reported in standard units where the diameter  $\sigma$  and mass  $m$  of a sphere, as well as the thermal energy  $k_B T$ , where  $k_B$  is the Boltzmann constant and  $T$  is the temperature, are all 1.) Analogously, the depletion force between a wall and a sphere can be derived from a density profile. We show the

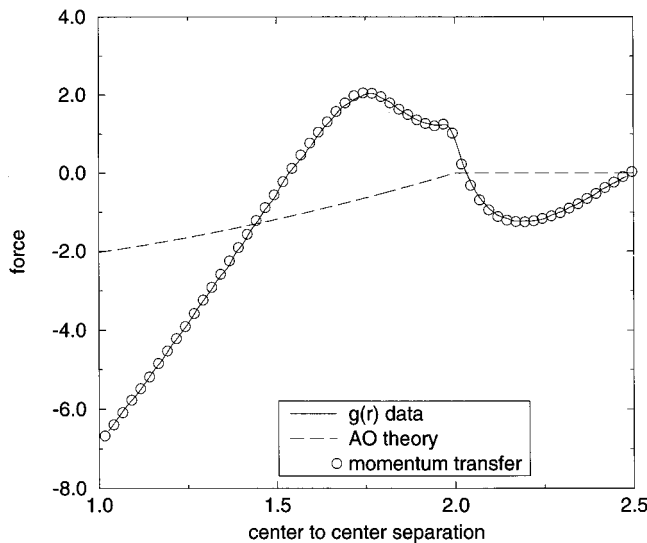


FIG. 1. Depletion force as a function of the distance between two hard spheres in a mixture of other hard spheres of the same size at a packing fraction  $\phi = 0.45$ .

force as a logarithmic derivative of the density as well as obtained from direct momentum transfer measurements in Fig. 2. Our simulations were carried out with 108 hard spheres at a packing fraction of about 0.45.

It is clear that, by ignoring the correlations in the subsystem of smaller particles, AO theory eliminates the possibility for the complex structure these forces really have. Yet naturally, as experimental conditions approach the ideal gas limit, the applicability of the predictions of the AO theory improves. In general, though, AO theory underestimates the magnitude of depletion forces at contact, ignores their oscillatory nature, and underestimates their range. These trends worsen as the density of the small particles increases.

Recently Kaplan, Faucheux, and Libchaber [17] reported a large discrepancy between their experiment and the AO prediction that surprisingly indicates that the AO theory

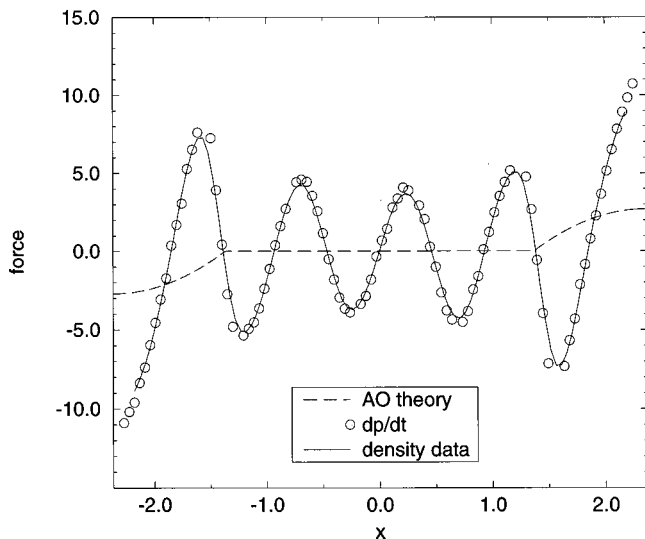


FIG. 2. Depletion force between a hard sphere and a hard wall in a mixture of other hard spheres for the system described in the text. The walls are placed such that the region accessible to the centers of the hard spheres ranges from  $-2.37$  to  $2.37$ .

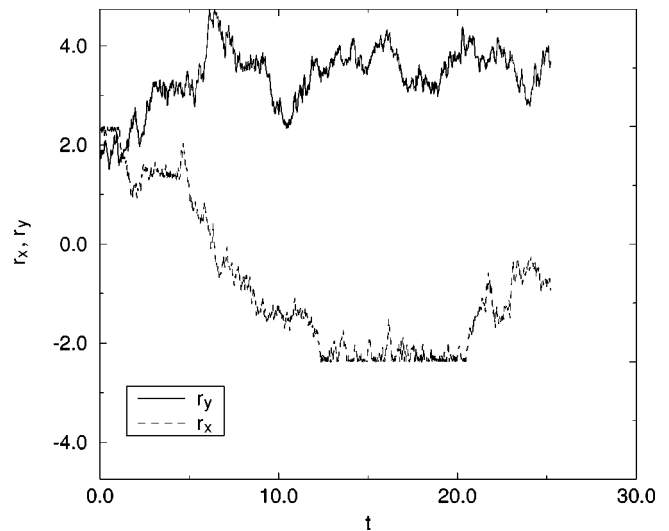


FIG. 3. Time series of particle displacements, parallel ( $y$ ) and perpendicular ( $x$ ) to the wall. Note that the time intervals in which the particle does not undergo significant parallel displacement do not correspond to trapping near a wall.

overestimates the contact value, and increasingly does so at higher densities. The method Kaplan, Faucheux, and Libchaber use for measuring entropic potentials is ingenious. By tracking the trajectory of a large sphere *parallel* to a wall, they probed the depth of the entropic potential well *perpendicular* to it. This method relies crucially on the dependence of the diffusion coefficient of a particle parallel to the wall on its distance from a wall [18]. We can test this assumption as our system satisfies this essential requirement [19] (even though the diffusion mechanism is fundamentally different) and we, therefore, performed a similar measurement in our simulations.

In Ref. [17], the depth of the potential well,  $\delta\mathcal{F}$ , near a wall was calculated from Kramers time  $\tau = \tau_F e^{\delta\mathcal{F}/k_B T}$ , where  $\tau_F$  is the inverse frequency of escape attempts and  $\tau$  is the escape time. The latter was identified with a crossover time below which diffusion, parallel to the wall, needed to be characterized by two distinct diffusion coefficients and above which one effective diffusion coefficient sufficed. When we estimate  $\tau$  according to this prescription, we obtain an unreasonably low value of 0.3 mean collision times, whereas an actual measurement of this time (by simply measuring the average time it takes for particles to escape from the potential well, associated with the first layer next to the wall, starting from a randomly chosen equilibrium configuration) gives a value larger by three to four orders of magnitude. We can conclude that, for our miniscale pure hard-sphere system, this type of analysis is not useful.

We can also readily follow the trajectories of our particles parallel to the wall as was done in the experiment—compare the top curve of our Fig. 3 to Fig. 3 of Ref. [17]. One might be tempted to find trappings perpendicular to the wall from these parallel trajectories following Ref. [17]. However, the true trapping events, as obtained from a direct study of the trajectories of the particles perpendicular to the walls, do *not* necessarily correspond to situations in which the parallel motion is inhibited. In other words, there can be significant motion parallel to the walls even when a particle remains within the first layer next to the wall. Likewise, the situation

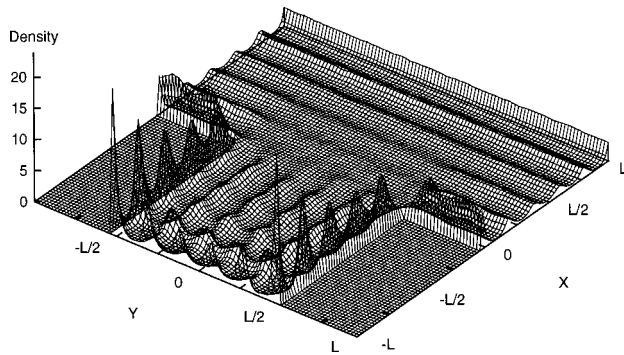
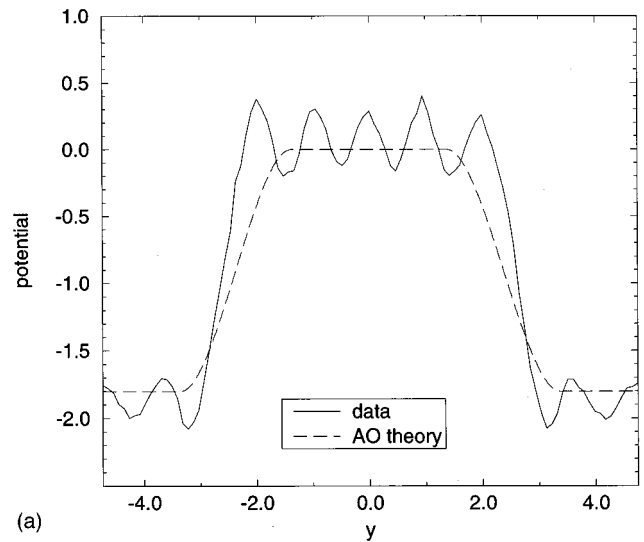


FIG. 4. Density profile for a hard-sphere fluid confined in a  $T$ -shaped channel with translational invariance in the  $z$  direction. To form the channel, thermal walls were placed in the  $y$ - $z$  plane at  $x = L + \sigma/2$ ;  $x = -L - \sigma/2$  for  $|y| < L/2 + \sigma/2$ ,  $x = -\sigma/2$  for  $|y| > L/2 + \sigma/2$ ; and in the  $x$ - $z$  plane at  $y = L/2 + \sigma/2$  and  $y = -L/2 - \sigma/2$ , both for  $x < -\sigma/2$ . Periodic boundary conditions were used otherwise.  $L = 4.74\sigma$ .  $\sigma$  is the hard-sphere diameter.

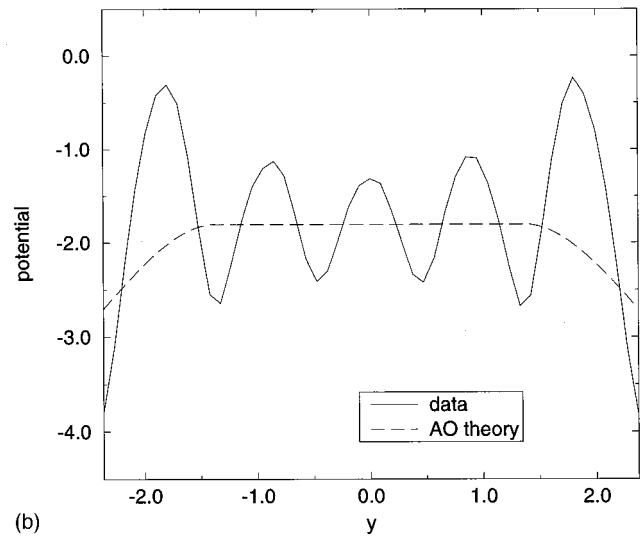
in which the parallel motion is arrested does not preclude significant perpendicular (to the wall) movement.

Depletion forces in complex geometries are beginning to receive increasing attention [10,11]. The AO calculations of entropic forces and potentials in these geometries are simple to carry out, while more precise predictions quickly become rather laborious and, to our knowledge, have not been successfully completed. By the virtue of having a simpler system to work with than a binary mixture, we can study depletion forces in regimes that have not been accessed before. Properly generalized, these results can be a useful guide to what to expect and search for in real systems. As an example, we obtained the equilibrium density for a system of 324 hard spheres at a packing fraction of about 0.45 in a  $T$ -shaped channel (see Fig 4). For this system, the potential near step edges and corners (see Fig. 4) is of principal interest and is shown in Fig. 5. A comparison with the AO prediction is also shown in the figure. The potential barrier repelling a hard sphere from a step edge is simply a reflection of the density decrease near it. Analogously, the potential minimum attracting particles towards a corner and the sharp increase in density there are different manifestations of the same effect. The earlier conclusions that we drew about the differences between AO theory and more precise simulations are valid here as well.

Yet, an interesting and fundamentally important feature of depletion forces manifests itself already in the AO approach—depletion forces need not be pairwise additive. In the AO approach, the force between two particles arises from the overlap of excluded volumes. Three-body effects become relevant when the hard spheres are considered in configurations in which their pairwise overlap volumes themselves overlap, resulting in an overcounting of the actual overlap volume. An example would be a configuration where three spheres are located at the vertices of an imaginary equilateral triangle of edge equal to the sphere diameter. The AO prediction for this geometry can be easily calculated. For the packing fraction  $\phi = 0.45$ , the AO two-body force at two-sphere contact is  $F_{AO} = -2.0$ . If forces were additive, the magnitude of the total force on a sphere in this triangular configuration would be  $2F_{AO} \cos(\pi/6) = -3.5$ . Instead,



(a)



(b)

FIG. 5. (a) The effective potential along  $x=0$  (see Fig. 4), showing a significant barrier at the edge. (b) The effective potential for  $x=-L$  (see Fig. 4), displaying a minimum in the corner.

when all overlap volumes are correctly accounted for, an AO-like analysis predicts a force of  $-2.9$ . The *exact* three-body force can, in principle, be found from a three-point correlation function, but obtaining reliable statistics for this measurement is rather time consuming. Instead, we prepared the described triangular configuration and measured the momentum transfer on each of the spheres in a simulation. The two-body force at contact for  $\phi = 0.45$  is  $F_{sim} = -6.8$  (see Fig. 1). The actual measured force,  $-10.0$ , is again noticeably lower than the additive pairwise force:  $2F_{sim} \cos(\pi/6) = -11.8$ . Indeed, the three-body component for our system of hard spheres is a significant percentage of the total force [9]. Pairwise additivity of forces is an integral part of many theories. When depletion forces are considered, this crucial property cannot be taken for granted.

This work was supported by the NSF GRT Program and funds from NASA, Center for Academic Computing at Penn State, and the Petroleum Research Fund, administered by the American Chemical Society.

- [1] S. Sanyal, N. Easwar, S. Ramaswamy, and A. K. Sood, *Europhys. Lett.* **18**, 107 (1992).
- [2] A. Imhof and J. K. G. Dhont, *Phys. Rev. Lett.* **75**, 1662 (1995).
- [3] P. Bartlett, R. H. Ottewill, and P. N. Pusey, *Phys. Rev. Lett.* **68**, 3801 (1992).
- [4] P. D. Kaplan, J. L. Rouke, A. G. Yodh, and D. J. Pine, *Phys. Rev. Lett.* **72**, 582 (1994).
- [5] J. Janzen and D. E. Brooks, *Clin. Hemorheol.* **9**, 695 (1989).
- [6] Y. Mao, M. E. Cates, and H. N. W. Lekkerkerker, *Physica A* **222**, 10 (1995).
- [7] P. Attard and G. N. Patey, *J. Chem. Phys.* **92**, 4970 (1990).
- [8] R. Dickman, P. Attard, and V. Simonian, *J. Chem. Phys.* **107**, 205 (1997).
- [9] T. Biben, P. Bladon, and D. Frenkel, *J. Phys.: Condens. Matter* **8**, 10 799 (1996). As pointed out in this paper, three-body effects became less significant as the large-sphere–small-sphere diameter ratio increases.
- [10] A. D. Dinsmore, A. G. Yodh, and D. J. Pine, *Nature (London)* **383**, 239 (1996).
- [11] A. D. Dinsmore, D. T. Wong, P. Nelson, and A. G. Yodh, *Phys. Rev. Lett.* **80**, 409 (1998).
- [12] S. Asakura and F. Oosawa, *J. Chem. Phys.* **22**, 1255 (1954); S. Asakura and F. Oosawa, *J. Polym. Sci.* **33**, 183 (1958).
- [13] X. Ye, T. Narayanan, P. Tong, and J. S. Huang, *Phys. Rev. Lett.* **76**, 4640 (1996).
- [14] Y. N. Ohshima, H. Sakagami, K. Okumoto, A. Tokoyoda, T. Igarashi, K. B. Shintaku, S. Toride, H. Sekino, K. Kabuto, and I. Nishio, *Phys. Rev. Lett.* **78**, 3963 (1997).
- [15] J.-P. Hansen and I. R. McDonald, *Theory of Simple Liquids* (Academic Press, London, 1986).
- [16] M. P. Allen and D. J. Tildesley, *Computer Simulation of Liquids* (Clarendon Press, Oxford, 1990).
- [17] P. D. Kaplan, L. P. Faucheux, and A. J. Libchaber, *Phys. Rev. Lett.* **73**, 2793 (1994).
- [18] L. P. Faucheux and A. J. Libchaber, *Phys. Rev. E* **49**, 5158 (1994).
- [19] In our system of hard spheres between hard walls, we measure the parallel-to-the-wall diffusion coefficient to be  $0.0280 \pm 0.0005$  in the first layer and  $0.0350 \pm 0.0010$  in the interior.